



Material and structural performance evaluation of recycled PET fiber reinforced concrete

Sung Bae Kim^a, Na Hyun Yi^a, Hyun Young Kim^a, Jang-Ho Jay Kim^{a,*}, Young-Chul Song^b

^a School of Civil and Environmental Engineering, Yonsei University, Concrete Structural Engineering Laboratory, A360, Engineering, Building #A, 134 Shinchon-dong, Seodaemun-gu, Seoul 120-749, South Korea

^b Structure and Assessment Group, Korea Electric Power and Research Institute, 103-16 Munji-Dong, Yuseong-Gu, Daejeon 305-380, South Korea

ARTICLE INFO

Article history:

Received 10 February 2009

Received in revised form 2 November 2009

Accepted 3 November 2009

Available online 10 November 2009

Keywords:

Recycle
PET fiber
PP fiber
Drying shrinkage
Cracking
Concrete
Ductility

ABSTRACT

Most PET bottles used as beverage containers become waste after their usage, causing environmental problems. To address this issue, a method to recycle wasted PET bottles is presented, in which short fibers made from recycled PET are used within structural concrete. To verify the performance capacity of recycled PET fiber reinforced concrete, it was compared with that of polypropylene (PP) fiber reinforced concrete for fiber volume fractions of 0.5%, 0.75%, and 1.0%. Appropriate tests were performed to measure material properties such as compressive strength, elastic modulus, and restrained drying shrinkage strain. Flexural tests were performed to measure the strength and ductility capacities of reinforced concrete (RC) members cast with recycled PET fiber reinforced concrete. The results show that compressive strength and elastic modulus both decreased as fiber volume fraction increased. Cracking due to drying shrinkage was delayed in the PET fiber reinforced concrete specimens, compared to such cracking in non-reinforced specimens without fiber reinforcement (NF), which indicates crack controlling and bridging characteristics of the recycled PET fibers. Regarding structural member performance, ultimate strength and relative ductility of PET fiber reinforced RC beams are significantly larger than those of companion specimens without fiber reinforcement.

© 2009 Elsevier Ltd. All rights reserved.

1. Introduction

Concrete is the most widely used construction material in the world due to its high compressive strength, long service life, and low cost. However, concrete has inherent disadvantages of low tensile strength and crack resistance. To improve such weaknesses of the material, numerous studies on fiber reinforced concrete have been performed. The research results show that concrete reinforced with short plastic fibers drastically improves the performance of concrete and negates its disadvantages such as low tensile strength, low ductility, and low energy absorption capacity [1–7]. Polypropylene (PP), polyethylene (PE), polyvinyl alcohol (PVA), polyvinyl chloride (PVC), nylon, aramid, and polyesters are commonly used short plastic fibers in concrete members [7–9]. Among these materials, PP fibers are one of the most widely used for construction applications such as in shotcrete tunnel linings, blast resistant concrete, overlays, and pavements [10,11].

Polyethylene terephthalate (PET) is one of the most important and extensively used plastics in the world, especially for manufacturing beverage containers. The current worldwide production of

PET exceeds 6.7 million tons/year and shows a dramatic increase in the Asian region due to recent increasing demands in China and India [12]. In Korea, the production of PET bottles has grown to 130 thousand tons/year [13]. However, most PET bottles used as beverage containers are thrown away after single usage and disposed PET bottles are managed by landfill and incineration, which are causing serious environmental problems [14]. In order to recycle PET wastes, additional expenses are required for reprocessing. Also, color change and purity degradation limit the usage of recycled PET plastics for manufacturing new products [15]. Thus, a more effective, less costly solution is needed for PET bottle wastes.

One possible solution is using recycled PET as short fiber reinforcement in structural concrete. It can provide crack control and ductility enhancement for quasi-brittle concrete as well as mass consumption alternative, which is an important issue in the merit of recycling wasted materials. The current applications of recycled PET in the construction industry include their use as resin for polymer concrete and synthetic coarse aggregate for lightweight concrete [15–21].

In this study, the basic material properties and drying shrinkage resistance of concrete reinforced with recycled PET fibers are evaluated. These recycled PET fibers are produced from waste PET bottles, as described later in this paper. Also, experimental

* Corresponding author. Tel.: +82 2 2123 5802; fax: +82 2 364 1100.
E-mail address: jhkim@yonsei.ac.kr (J.H.J. Kim).

Table 1
Mix proportion of concrete.

Specimens	W/B	S/a (%)	Unit weight (kg/m ³)						Fiber volume fraction (%)	
			C	FA	W	S	G	AE	Recycled PET	PP
NF									–	–
RPET 0.5									0.5	–
RPET 0.75									0.75	–
RPET 1.0	0.41	43.8	355	40	161	775	994	2.37	1.0	–
PP 0.5									–	0.5
PP 0.75									–	0.75
PP 1.0									–	1.0



Fig. 1. Manufacturing process of recycled PET fibers.

study of the strength, ductility and failure mode of recycled PET fiber reinforced RC beams is performed. Based on the study results, which include comparisons with specimens containing PP fiber reinforcement, the application of recycled PET fiber reinforced concrete as a structural material is evaluated.

2. Materials

2.1. Concrete mix

Mix proportions for the concrete are indicated in Table 1. Ordinary Portland cement with a density of 3.15 g/cm³ and Blaine fineness of 3.49×10^3 cm²/g was used, along with a 10.1% substitution by weight with fly ash (FA). This provided a water-to-binder ratio (W/B) of 0.41. Crushed gravel with maximum size of 25 mm was used for coarse aggregate; river sand was used for fine aggregate. An air-entraining/water-reducing agent was added to achieve an air content of $4.5 \pm 1.5\%$ and appropriate workability.

2.2. Recycled PET fiber

In this study, recycled PET plastic sheeting produced from waste PET bottles (supplied in rolls, as seen in Fig. 1) is used. The plastic sheet is slit into thin strands, producing straight continuous fibers. However, straight plastic fibers typically have low bond strength with the concrete matrix, and therefore do not provide the intended crack resisting ability of fiber concrete. To improve bond strength between the recycled PET fibers and concrete matrix, the fiber geometries are deformed into one of several patterns. Generally, the manufactured fibers are of crimped, twisted, and embossed patterns. For this study, embossed fibers were chosen for their superior bond properties for this type of fiber material [22]. Different deformation patterns have been found effective for other fiber materials [23].

After the recycled PET strands are given the desired surface configuration, the fiber surface is coated with maleic anhydride grafted polypropylene. The surface coating improves the bonding strength and dispersion characteristics of the recycled PET fiber [24]. After the coating process, the strands are chopped into desired fiber length. Figs. 1 and 2 show the manufacturing system of recycled PET fibers. To verify the properties of recycled PET fiber, recycled PET fiber is compared with similar size PP fiber. The PP fiber used in the study is a commercial product (Contechsnc HPPF, produced by CONTECSNC [25]) and the surface configuration is of crimped type. Fig. 3a and b shows images of the manufactured recycled PET and purchased PP fibers, respectively. The basic properties of both types of fibers are indicated in Table 2 [24].

The primary variables in this study are (a) synthetic fiber type and (b) fiber volume fraction. Fiber volume fractions were chosen as 0.5%, 0.75% and 1.0%, as indicated in Table 1.

3. Material property tests

3.1. Compressive strength and elastic modulus

Tests for compressive strength and elastic modulus were performed on bare recycled PET and PP fiber reinforced concrete specimens. Fiber concrete cylinders of 100 × 200 mm were tested at an age of 28 days. These cylindrical specimens were tested by a universal testing machine (UTM) with a maximum load capacity of 2000 kN. The results for each specimen type are based on an average value of three replicate specimens.

Compressive strength and elastic modulus experiments are performed according to Korean Standard 2405 and 2438 test methods, respectively [26,27]. Static elastic modulus, applicable within the customary working stress range of 0–40% of ultimate concrete strength, was calculated as follows.

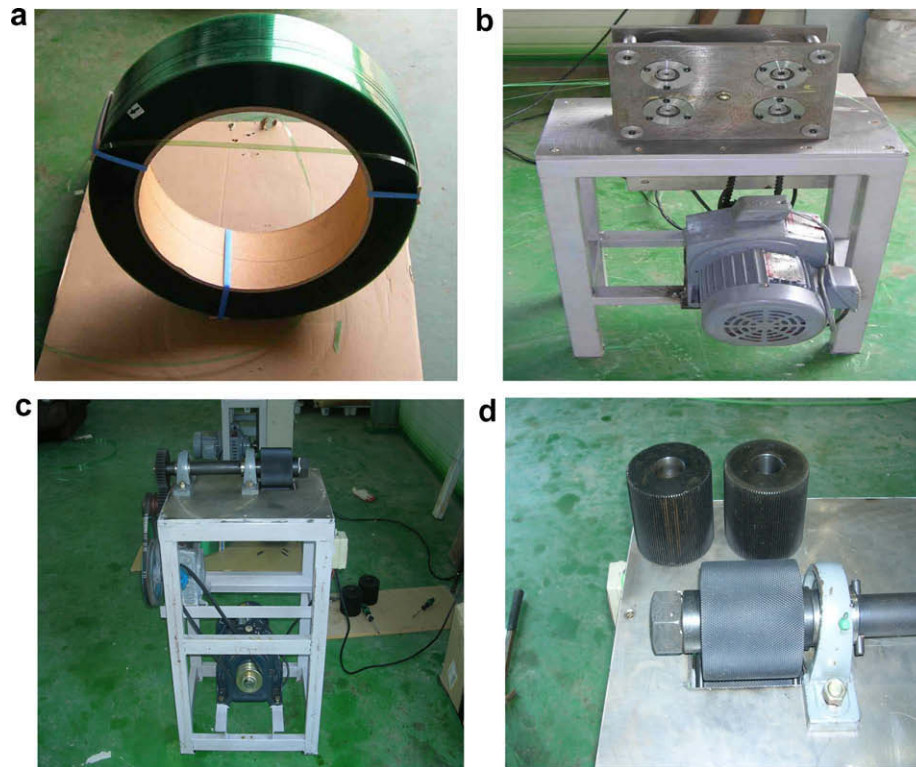


Fig. 2. Manufacturing system of recycled PET fibers; (a) recycled PET sheet; (b) slitting machine; (c) deforming machine; (d) gear of deforming machine.

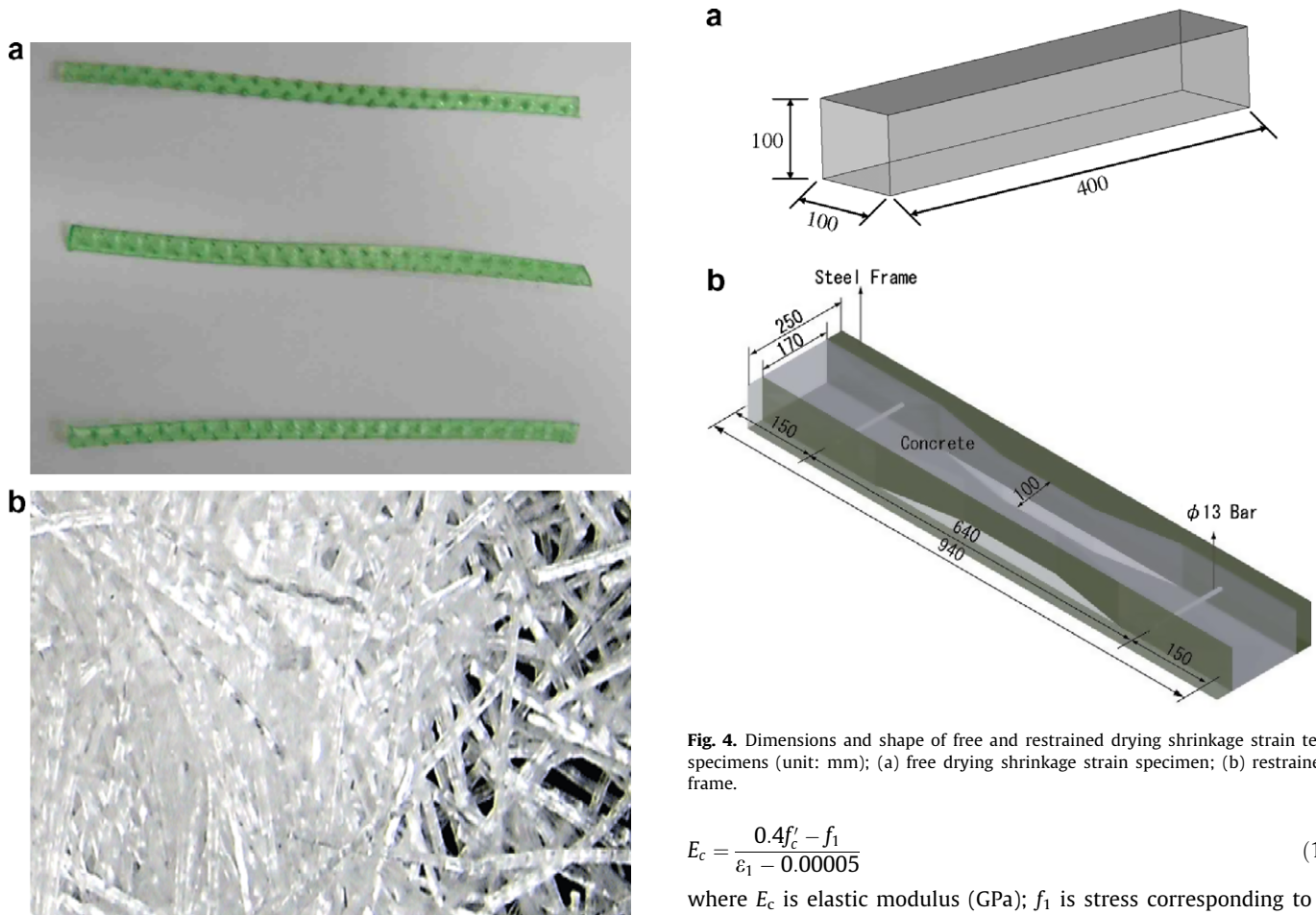


Fig. 3. Geometry of the recycled PET fiber and PP fiber; (a) RPET fiber; (b) PP fiber.

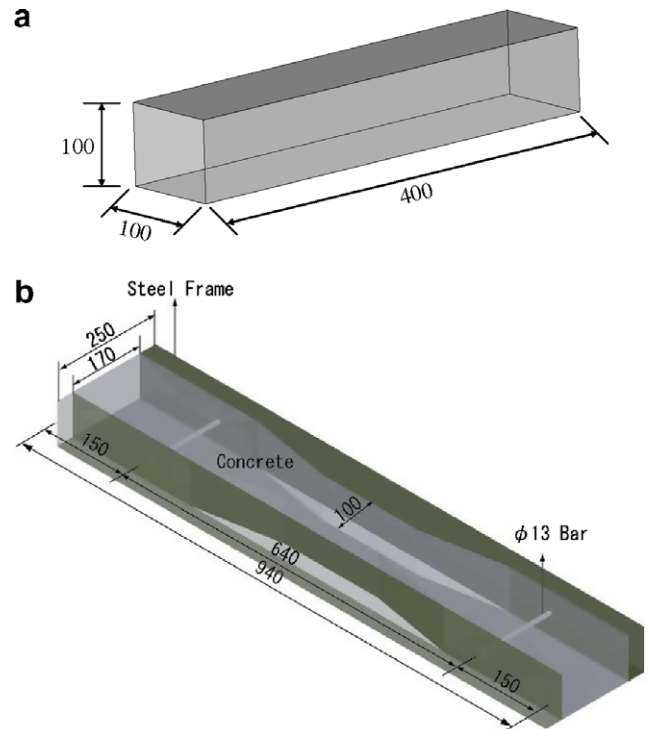


Fig. 4. Dimensions and shape of free and restrained drying shrinkage strain test specimens (unit: mm); (a) free drying shrinkage strain specimen; (b) restrained frame.

$$E_c = \frac{0.4f'_c - f_1}{\varepsilon_1 - 0.00005} \quad (1)$$

where E_c is elastic modulus (GPa); f_1 is stress corresponding to a longitudinal strain of 0.00005 (MPa); ε_1 is the longitudinal strain produced by stress $0.4f'_c$.

Table 2

Properties of synthetic fibers [24].

Fibers	Type	Dimension (mm)	Length (mm)	Density (g/cm ³)	Elastic modulus (MPa)	Tensile strength (MPa)	Ultimate elongation (%)
Recycled PET	Embossed	0.2 × 1.3	50	1.38	1.02 × 10 ⁴	420.7	11.2
PP	Crimped	0.38 × 0.9	50	0.91	6.00 × 10 ³	550.0	15.0

3.2. Free and restrained drying shrinkage strain tests

To analyze the effect of recycled PET fiber on drying shrinkage cracking of fiber reinforced concrete, free and restrained drying shrinkage strain experiments are performed according to Korean Standard 2595 test method for drying shrinkage cracking of restrained concrete [28]. The dimensions and shape of the specimen for free and restrained drying shrinkage strain tests are shown in Fig. 4.

The specimens were manufactured and wet-cured until testing. Curing temperature was 20 ± 1 °C with humidity of $60 \pm 5\%$. Removal of formwork was performed after 7 days from casting. To measure restrained drying shrinkage strain after removal of the formwork, concrete and steel plate gauges are used. Concrete strain was measured at the center of the upper surface of the concrete specimen and strain in the steel restraining plate was mea-

sured at the center of the plate length. The occurrence of full through cracks was checked daily; cracking location and time were recorded for each specimen.

3.3. Experimental results and discussion

3.3.1. Compressive strength and elastic modulus

Fig. 5a and b presents the compressive strength and elastic modulus test results, respectively, for 0.5%, 0.75% and 1.0% fiber volume fractions. The recycled PET and PP fiber-reinforced specimens exhibited strength decreases of 1–9% and 1–10%, respectively, compared to the non-reinforced specimens. Other studies have found lower 28-day compressive strengths of short synthetic fiber reinforced concrete, compared to strengths of concretes not reinforced with fibers [29]. As expected for the addition of low modulus synthetic fibers, the recycled PET and PP concrete specimens showed lower elastic moduli than those of the unreinforced specimens. Elastic modulus decreased with increasing fiber content.

3.3.2. Free and restrained drying shrinkage strain tests

The measured free drying shrinkage strain is shown in Fig. 6. The non-reinforced specimen showed the least free drying shrinkage strain, whereas recycled PET and PP fiber reinforced concrete specimen showed 8–25% higher strain. The larger strains are likely due to modification of the pore volume and pore structures through the introduction of fibers into the mix. This logic has been confirmed by Rebeiz et al. [15] where large volume of air voids in concrete due to excessive amount of synthetic fiber volume fraction was found to cause more drying shrinkage strain in the material. However, the RPET 0.5 specimen showed the largest free drying shrinkage strain and PP fiber-reinforced specimens showed decreasing strain as fiber volume fraction increased.

The measured restrained drying shrinkage strain versus curing time is shown in Fig. 7. The time of full through cracking of individual specimens is tabulated in Table 3. Full through cracks occurred on 14 and 25 days in the non-reinforced and RPET 1.0 specimens,

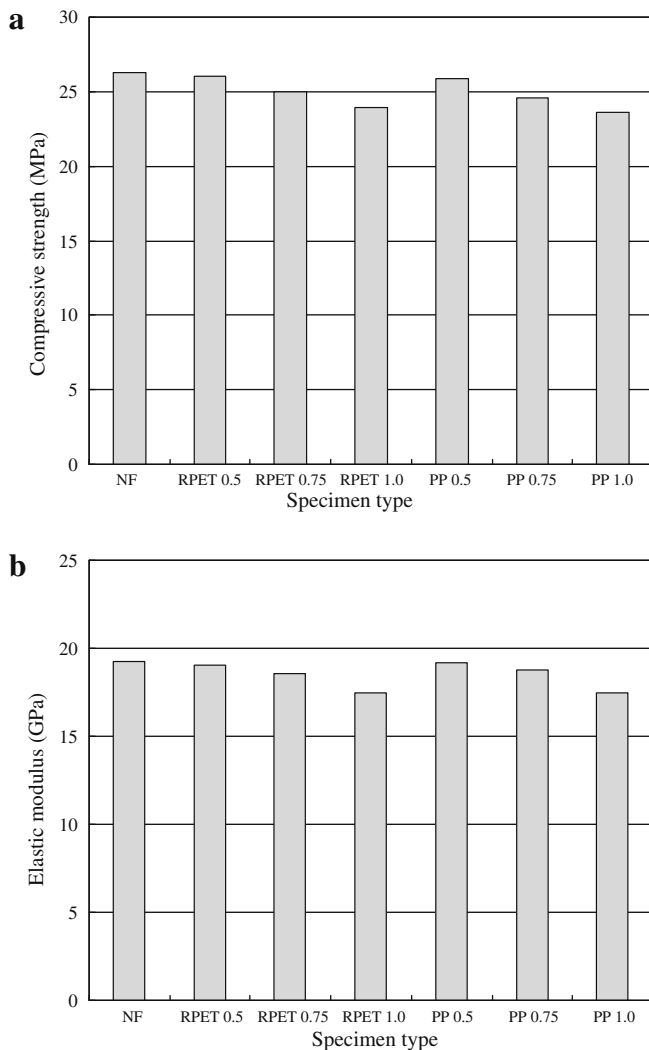


Fig. 5. Compressive strength and elastic modulus for fiber volume fraction of NF, RPET, and PP specimens; (a) compressive strength; (b) elastic modulus.

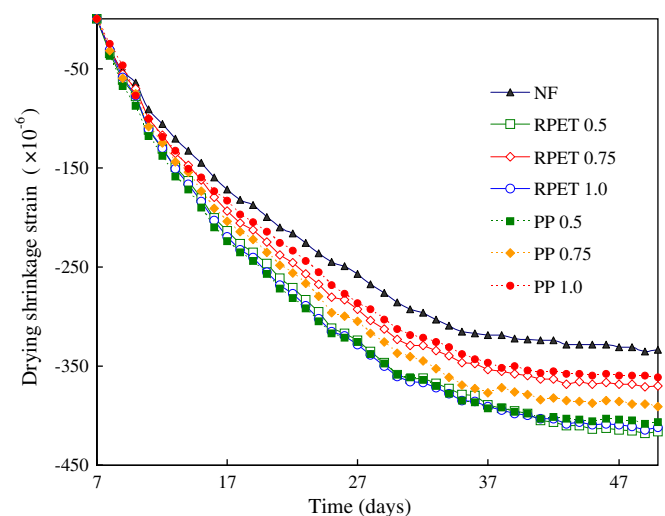


Fig. 6. Free drying shrinkage strains of NF, RPET, and PP specimens.

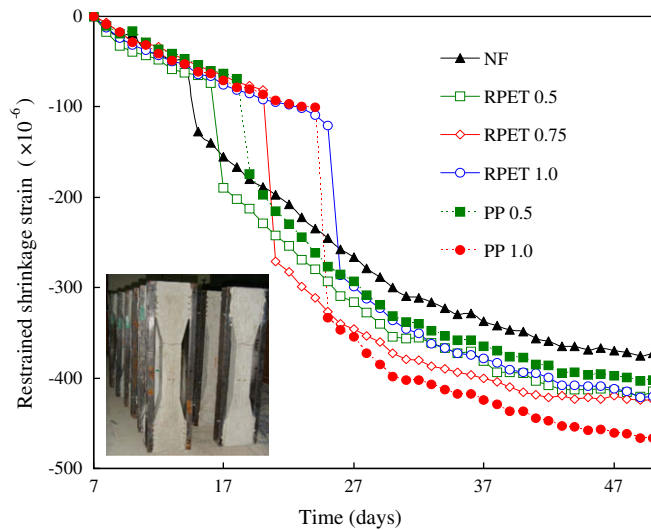


Fig. 7. Results of restrained drying shrinkage strains of NF, RPET, and PP specimens in restrained concrete.

respectively, which are the minimum and maximum cracking times observed among all specimens. Crack occurrence time appears to be delayed as the fiber volume fraction increased. In conclusion, the addition of recycled PET fibers in concrete improved concrete crack controlling capacity, thereby delaying crack occurrence time.

Restrained tensile strain of concrete can be defined as the difference between free and restrained drying shrinkage strains.

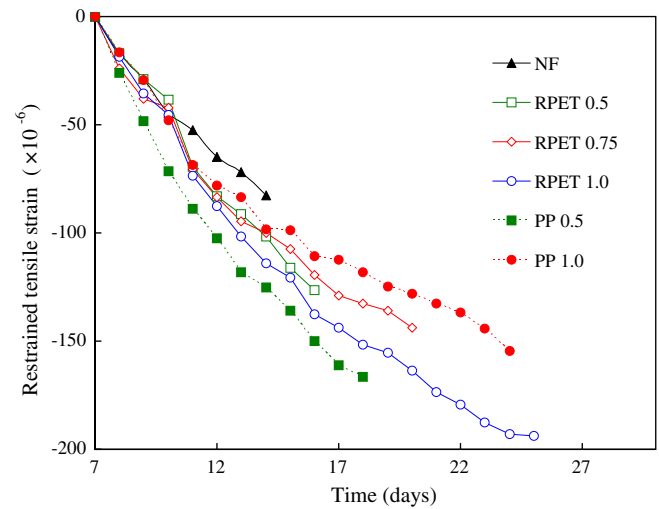



Fig. 8. Restrained tension strains of NF, RPET, and PP specimens.

Generally, when restrained tensile strain of concrete is higher, it is more susceptible to cracking [30]. In this study, however, the non-reinforced and RPET 1.0 specimens that had the minimum and maximum restrained tensile strains cracked earliest and latest, respectively, as shown in Fig. 8. The likely reason for this inverse trend is that the crack bridging capabilities of short fiber reinforcement are activated when significant strains and micro-cracks are formed, causing the delay in macro-cracking.

Table 3
Result of drying shrinkage cracking time and location.

Specimens	Shrinkage crack time (days)	Cracking point
NF	14	
RPET 0.5	16	
RPET 0.75	20	
RPET 1.0	25	
PP 0.5	19	
PP 1.0	24	

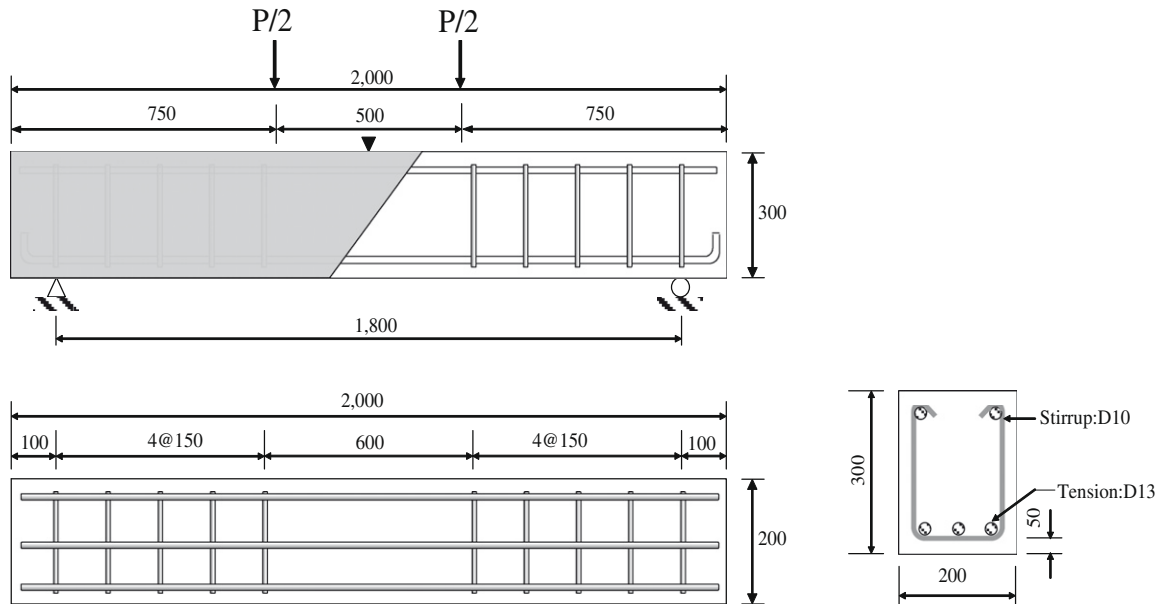


Fig. 9. Dimensions and details of RC beam specimen (unit: mm).

4. Structural member capacity test

To simulate realistic stress conditions in structures, RC beam specimens were designed to apply both shear and flexure stresses using a span to depth ratio of 2.6. The specimens were tested under 4-point loading to enforce this condition. However, the specimens were designed to fail in a flexural rather than shear mode. The overall ductility and energy absorbing capacities were calculated.

4.1. Flexural strength test

A total of seven specimens were tested after 28 days from casting. The specimens were reinforced with three D13 bars as tensile reinforcement, D10 bars as compressive reinforcement, and 10 mm diameter shear stirrups with 150 mm spacing. Fig. 9 shows the dimensions and details of the beam specimens. Fig. 10 shows the test set-up. RC beam specimens with hinge-roller supports were tested using a UTM with a maximum load capacity of 2000 kN. The load was applied as stroke control loading. The rate of vertical displacement at the mid-span was 0.025 mm/s. Before loading, a strain gauge was attached at the bottom surface of the concrete beam to measure the tensile strain. To obtain an accurate deflection reading, a Linear Variable Differential Transducer (LVDT) was mounted at the mid-span. Crack initiation and propagation were monitored by visual inspection during testing, and the crack patterns were marked.

4.2. Experimental results and discussion

4.2.1. Load–deflection results

The measured load–deflection relations from the RC beam tests are shown in Fig. 11. The results showed that the elastic behavior of all specimens before cracking was similar even though the fiber volume fractions were different. Before the yielding of tensile reinforcement, initiation of cracks occurred earlier in the fiber reinforced concrete specimens than in the specimens without fibers, except in PP 0.5 specimens. However, once the re-

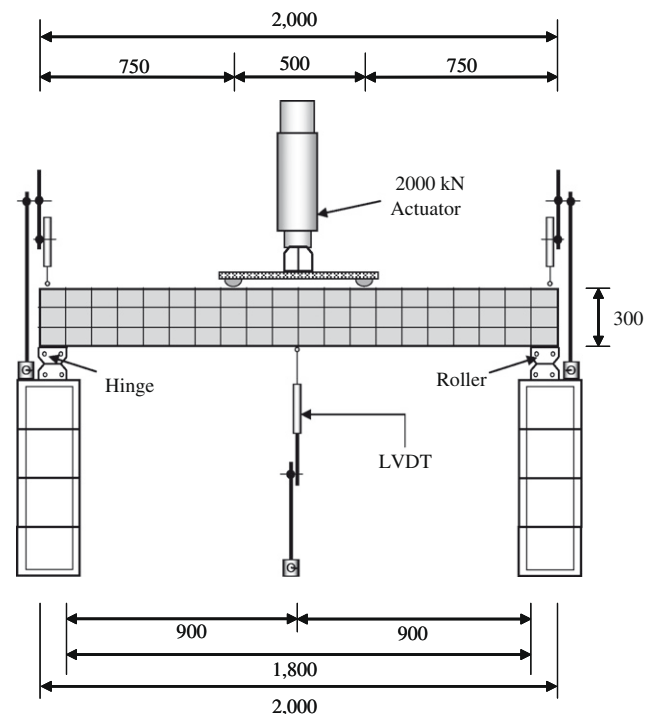


Fig. 10. Test set-up and data acquisition locations (unit: mm).

bar yields, the fiber reinforced concrete showed better crack resistance and strain-hardening capacities than the specimens without fibers. Due to the increase in crack resistance, the cracking and spalling of the concrete cover and reinforcement debonding failure due to macro-crack propagation are delayed, which stabilizes the overall behavior of the structural RC member. In turn, this delay increases the overall flexural strength and ductility of the RC member.

The calculated flexural strength from the test data is tabulated in Table 4. As shown in the table, the RPET specimens

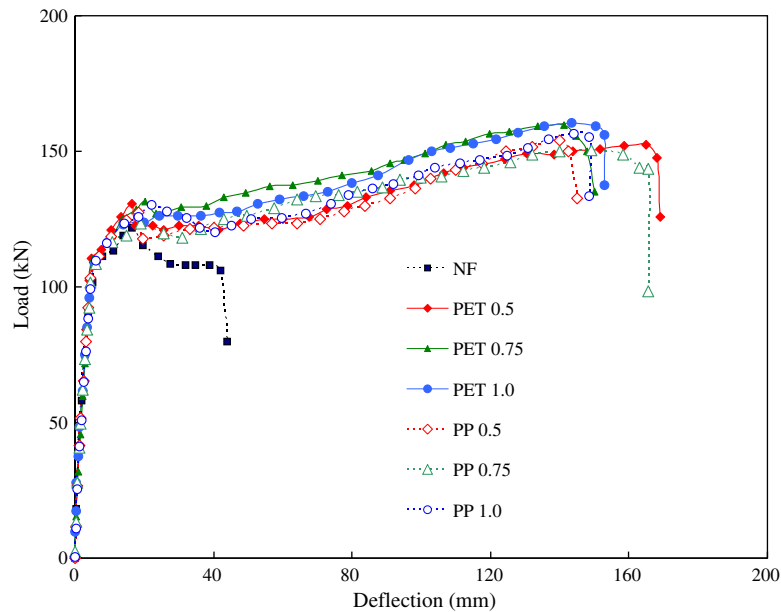


Fig. 11. Load–deflection curves of NF, RPET, and PP specimens at the age of 28 days.

Table 4

Summarized flexural strength test results.

Specimens	P_{cr} (kN)	Δ_{cr} (mm)	P_y (kN)	Δ_y (mm)	P_u (kN)	P_u/P_{unf} (%)	Δ_u (mm)
NF	32.6	1.01	101.4	4.80	121.6	100	16.94
RPET 0.5	24.8	0.43	109.0	4.52	152.6	125.5	165.0
RPET 0.75	22.0	0.51	108.8	4.67	159.8	131.4	141.36
RPET 1.0	32.4	0.62	107.8	5.31	160.4	131.9	143.36
PP 0.5	32.8	0.75	108.2	4.93	154.0	127.0	140.07
PP 0.75	28.0	0.69	106.3	5.21	150.4	123.7	149.16
PP 1.0	25.6	0.61	106.6	4.71	156.6	128.6	144.22

with fiber volume fractions of 0.5%, 0.75%, and 1.0% had ultimate strength increases of 25%, 31%, and 32%, respectively, compared to the concrete specimens without fiber reinforcement. The PP fiber reinforced concrete specimens showed similar trends observed in recycled PET fiber reinforced concrete specimens.

4.2.2. Cracking modes for the beams

Crack distributions at failure for all of the tested specimens are shown in Fig. 12, where the solid and dotted lines represent cracks that are formed during pre- and post-yielding stages of the tensile reinforcement, respectively. The control specimen without fiber reinforcement showed a general RC flexural failure behavior as expected.

In this study, the specimens without fiber reinforcement were designed to fail by yielding of the tensile reinforcement, which is proved by the crack distributions shown in Fig. 12. However, the recycled PET and PP fiber-reinforced specimens ultimately failed by both concrete compression and yielding of the tensile reinforcement. The load–deflection diagram shows that the maximum mid-span deflection is approximately 400% larger in the fiber-reinforced specimens than the specimens without fibers, as shown in Fig. 11. The images in Fig. 13 also show the significant difference in member rotation between fiber-reinforced specimens and those without fiber reinforcement.

4.2.3. Ductility and ultimate failure energy capacity

To quantify the load–deflection capacity of the tested specimens, the ductility index and ultimate failure energy capacity are used. The deflection ductility index can be defined as

$$\mu_{\Delta} = \frac{\Delta_u}{\Delta_y} \quad (2)$$

where Δ is the deflection of the member and indices u and y correspond to the ultimate and yield conditions, respectively. Ultimate failure energy capacity of a member is defined as the area under load–deflection relationship curve.

The ductility indices and energy capacities for tested beams are tabulated in Table 5. As shown in the table, the recycled PET fiber reinforced concrete specimens have a relative ductility index of 7.65–10.34, which is approximately 7–10 times greater than that of the specimens without fiber reinforcement. The calculated ultimate failure energy capacity of fiber reinforced concrete members are approximately 4.0–4.8 times greater than those of the specimens without fiber reinforcement. Notably, the RPET 0.5 specimen had the largest energy capacity and ductility index results, suggesting that there is an optimal fiber volume fraction for a given mix design and production process.

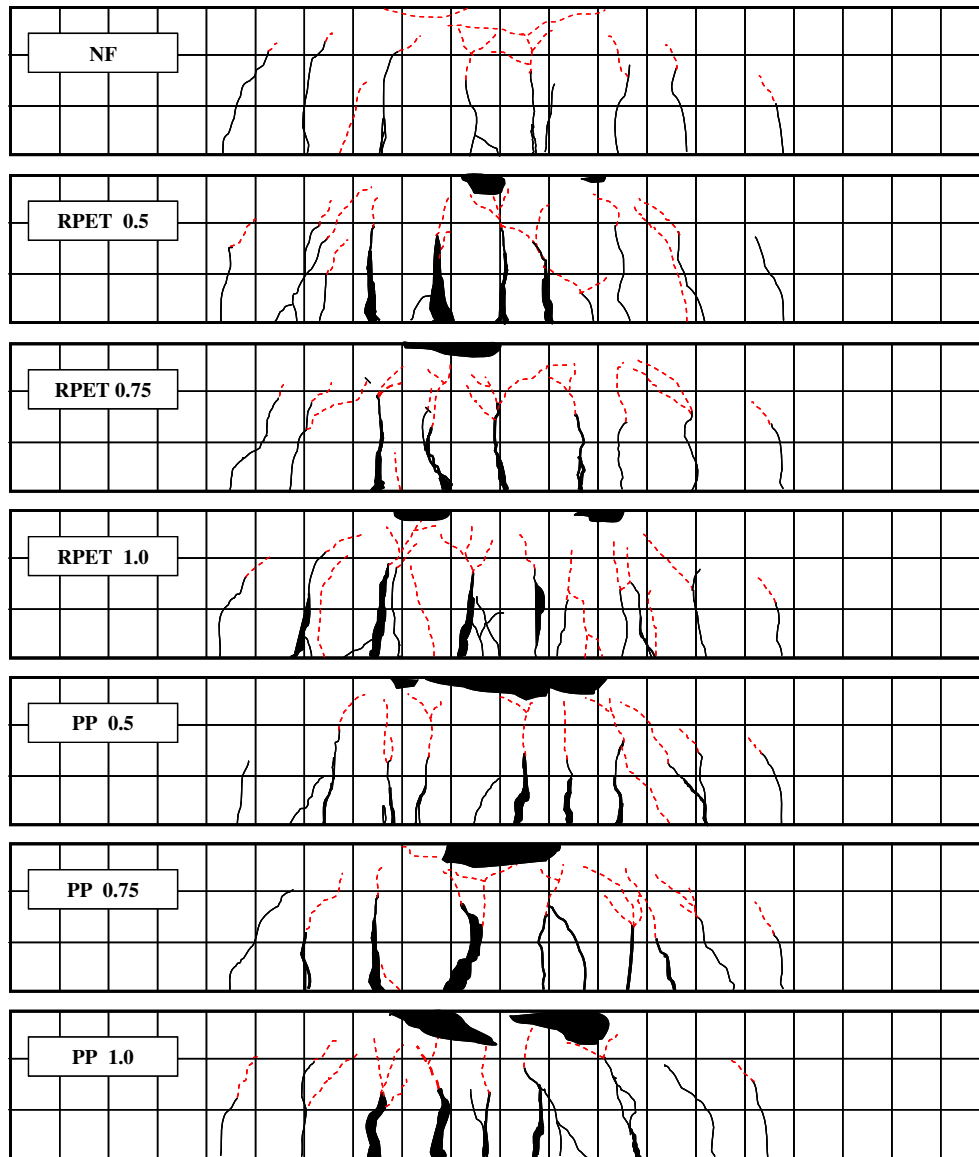


Fig. 12. Crack patterns at ultimate failure of NF, RPET, and PP RC specimens.

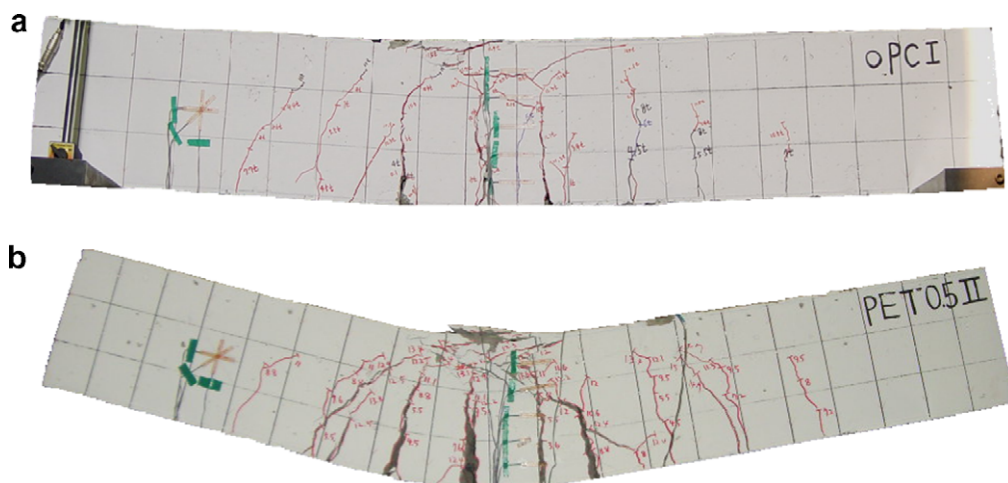


Fig. 13. Failure modes of RC beams; (a) NF RC beam; (b) RPET fiber reinforced RC beam.

Table 5

Calculated ductility index and energy capacity of test specimens.

Specimens	Δ_y (mm)	Δ_u (mm)	Ductility index (Δ_u/Δ_y)	Relative ductility index	Energy capacity (kN m)	Relative energy capacity
NF	4.80	16.94	3.53	1	4.64	1
RPET 0.5	4.52	165.0	36.50	10.34	22.50	4.85
RPET 0.75	4.67	141.36	30.27	8.58	20.87	4.30
RPET 1.0	5.31	143.36	27.00	7.65	21.05	4.34
PP 0.5	4.93	140.07	28.41	8.05	18.74	4.04
PP 0.75	5.21	149.16	28.63	8.11	21.77	4.69
PP 1.0	4.71	144.22	30.62	8.67	19.64	4.23

5. Conclusions

In this experimental study, recycled PET fibers have been added to structural concrete as a means for improving material and structural performance. The ecological benefit of effectively utilizing this waste material is another prime motivation for this work. The conclusions are as follows:

- (1) From the material property tests, recycled PET fiber reinforced concrete exhibited a slight decrease in compressive strength and elastic modulus as the fiber volume fraction increased. The recycled PET and PP fiber-reinforced specimens showed compressive strength decreases of 1–9% and 1–10%, respectively, compared to specimens without fiber reinforcement.
- (2) Free and restrained shrinkage strain tests were performed to evaluate the crack resistance of the concrete specimens. The results showed that free drying shrinkage strain increased for recycled PET fiber reinforced concrete specimens compared to that of the specimens without fiber reinforcement. For the case of restrained shrinkage, however, the fibers enhanced tensile resistance and delayed macro-crack formation.
- (3) Increased ductility and ultimate strength were observed for RC beams produced with the recycled PET fiber and PP fiber reinforced concretes. Ductility and ultimate load capacity increased by a maximum of 1000% and 30%, respectively, when comparing the recycled PET fiber-reinforced specimens to those without fiber reinforcement. Similar improvements were seen for the additions of PP fiber reinforcement.
- (4) The recycled PET fiber reinforced concrete specimens failed by both concrete compression and yielding of the tensile reinforcement. This behavior can occur when the effective load resisting cross-section remains approximately equivalent to the original cross-section, bonding between the rebar and concrete remains sufficiently intact to produce uniformity, and cracks formed during the initial stages of loading are bridged by the short fibers randomly distributed within the member. The maximum mid-span deflection is approximately 400% larger in the fiber-reinforced specimens, relative to the specimens without fiber reinforcement.
- (5) The recycled PET fiber reinforced concrete specimens had relative ductility indices of approximately 7–10 times greater than those of the specimens without fiber reinforcement. Beyond a volume fraction of about 0.5%, however, the ductility index and energy capacity decrease as the fiber volume fraction increases.

Acknowledgments

This research was supported by the financial assistance from Korea Science and Engineering Foundation (KOSEF) (Grant No. R01-2008-000-1117601) and Center for Concrete Core from the Ministry of Construction and Transportation.

References

- [1] Banthia N, Sheng J. Fracture toughness of micro-fiber reinforced cement composites. *Cem Concr Comp* 1996;18(4):251–69.
- [2] Bayasi MZ, Zeng J. Composite slab construction utilizing carbon fiber reinforced mortar. *ACI Struct J* 1997;94(4):442–6.
- [3] Dwarakanath HV, Nagaraj TS. Deformational behavior of fiber-reinforced concrete beams in bending. *J Struct Eng ASCE* 1992;118(10):2691–8.
- [4] Mu B, Li Z, Peng J. Short fiber-reinforced cementitious extruded plates with high percentage of slag and different fibers. *Cem Concr Res* 2000;30(8):1277–82.
- [5] Li VC, Kanda T. Engineered cementitious composites for structural applications. *J Mater Civil Eng ASCE* 1998;10(2):66–9.
- [6] Kanda T, Li VC. Interface property and apparent strength of a high-strength hydrophilic fiber in cement matrix. *J Mater Civ Eng ASCE* 1998;10(1):5–13.
- [7] Li VC, Horii H, Kabele P, Kanda T, Lim YM. Repair and retrofit with engineered cementitious composites. *Eng Fract Mech* 2000;65(2–3):317–34.
- [8] Cengiz O, Turanli L. Comparative evaluation of steel mesh, steel fibre and high-performance polypropylene fibre reinforced shotcrete in panel test. *Cem Concr Comp* 2004;34(8):1357–64.
- [9] Zollo RF. Fiber-reinforced concrete: an overview after 30 years of development. *Cem Concr Comp* 1997;19(2):107–22.
- [10] Mwangi JPM. Flexural behavior of sisal fiber reinforced concrete beams. PhD thesis. University of California Davis; 2001.
- [11] Aulia TB. Effects of polypropylene fibers on the properties of high-strength concrete. *Leipzig Annu Civ Eng Rep* 2002;5:43–59.
- [12] Vinyl Environmental Council of Japan (JVEC); 2008. <<http://www.vec.gr.jp/enbi/seisan.htm>>
- [13] Korea PET Container Association (KPCA); 2008. <<http://www.kpcaa.or.kr>>
- [14] Korean Institute of Resources Recycling. Recycling white paper. Cheong Moon Gak; 2008 [in Korean].
- [15] Rebeiz KS, Fowler DW, Paul DR. Recycling plastics in polymer concrete for construction applications. *J Mater Civ Eng ASCE* 1993;5(2):237–48.
- [16] Choi YW, Moon DJ, Chung JS, Cho SK. Effects of waste PET bottles aggregate on the properties of concrete. *Cem Concr Res* 2005;35(4):776–81.
- [17] Jo BW, Park SK, Park JC. Mechanical properties of polymer concrete made with recycled PET and recycled concrete aggregates. *Constr Build Mater* 2008;22(12):2281–91.
- [18] Jo BW, Tae GH, Kim CH. Uniaxial creep behavior and prediction of recycled PET polymer concrete. *Constr Build Mater* 2007;21(7):1552–9.
- [19] Rebeiz KS. Time-temperature properties of polymer concrete using recycled PET. *Cem Concr Compos* 1995;17(2):119–24.
- [20] Rebeiz KS, Fowler DW. Flexural strength of reinforced polymer concrete made with recycled plastic waste. *ACI Struct J* 1996;93(5):524–30.
- [21] Rebeiz KS, Serhal S, Fowler DW. Shear behavior of steel reinforced polymer concrete using recycled plastic. *ACI Struct J* 1993;90(6):675–82.
- [22] Kim JHJ, Park CG, Lee SW, Lee SW, Won JP. Effects of the geometry of recycled PET fiber reinforcement on shrinkage cracking of cement-based composites. *Compos Part B: Eng* 2008;39(3):441–50.
- [23] Kim D-J, Naaman AE, El-Tawil S. Comparative flexural behavior of four fiber reinforced cementitious composites. *Cem Concr Compos* 2008;30(10):917–28.
- [24] Won JP, Park CG, Kim HH, Lee SW. Effect of hydrophilic treatments of recycled PET fiber on the control of plastic shrinkage cracking of cement-based composites. *J Korean Soc Civ Eng* 2007;27(3A):413–9 [in Korean].
- [25] Concrete Technology System & Consultants (CONTECSNC); 2009. <<http://contechsnc.com>>.
- [26] KS F 2405. Method of test for compressive strength of concrete. Korea Standards Association; 2005 [in Korean].
- [27] KS F 2438. Testing method for static modulus of elasticity and poisson's ratio in compression of cylindrical concrete specimens. Korea Standards Association; 2002 [in Korean].
- [28] KS F 2595. Method of test for drying shrinkage cracking of restrained concrete. Korea Standards Association; 2004 [in Korean].
- [29] Bayasi Z, Zeng J. Properties of polypropylene fiber reinforced concrete. *ACI Mater J* 1993;90(6):605–10.
- [30] Ohno T, Uomoto T. Prediction of occurrence of cracks due to autogenous shrinkage and drying shrinkage. *Jpn Soc Civ Eng* 2000;49:29–44.